

# CHIRAL SYMMETRY AND THE SPECTRUM OF THE QCD DIRAC OPERATOR

J.J.M. VERBAARSCHOT

*Department of Physics  
SUNY at Stony Brook, Stony Brook, NY11790, USA*

According to the Banks-Casher formula the chiral order parameter is directly related to the spectrum of the Dirac operator. In this lecture, we will argue that some properties of the Dirac spectrum are universal and can be obtained from a random matrix theory with the global symmetries of the QCD partition function. In particular, this is true for the spectrum near zero on the scale of a typical level spacing. Alternatively, the chiral order parameter can be characterized by the zeros of the partition function. We will analyze such zeros for a random matrix model at nonzero chemical potential.

## 1. Introduction

Many phenomena in nuclear physics, as for example the lightness of the pion mass and the absence of parity doublets, can be explained by the assumption that chiral symmetry is spontaneously broken. This assumption has been confirmed by numerous lattice QCD simulations (for a review see [1,2]). However, these studies also show that chiral symmetry [3] is restored at a critical temperature of  $T_c \approx 140$  MeV. In spite of steady progress [4], the situation at nonzero baryon number density is much less clear [5]. It seems that the quenched approximation does not work [5,6], and the phase of the fermion determinant makes unquenched simulations virtually impossible.

The order parameter of the chiral phase transition is the chiral condensate. It is directly related to the spectral density of the Euclidean Dirac operator [7]. One of the questions we wish to address is to what extent the Dirac spectrum shows universal features which can be obtained from a Random Matrix Theory (RMT) with the global symmetries of the QCD partition function (chiral Random Matrix Theory (chRMT)). As is well-known from the study of complex systems [8], only correlations on a scale set by the eigenvalue spacing are given by RMT. Such correlations may be important in mesoscopic systems. Typical examples are a finite nucleus [9], small metallic particles [10], quantum dots and disordered wires (see [11] for a review). In particular, universal conductance fluctuations have been understood in the framework of RMT [12]. In

lattice QCD simulations, with a mesoscopic number of degrees of freedom, we expect to observe similar phenomena. In particular, in the mesoscopic range of QCD, for box size  $L$  given by [13]  $1/\Lambda \ll L \ll 1/m_\pi$ , we expect to obtain exact results from RMT ( $\Lambda$  is a typical hadronic scale and  $m_\pi$  is the pion mass).

In spite of its success in explaining mesoscopic phenomena, I wish to emphasize that there is no universality on a macroscopic scale and that RMT cannot be used to obtain quantitative predictions at this scale. (Note, however, [14–17].). This does not imply that RMT cannot be useful for the study of macroscopic phenomena. They have widely been used as *schematic* models for disorder, e.g., Anderson localization [18] and the Gross-Witten model [19]. Because of problems in simulating QCD at a nonzero baryon number density, chRMT is an ideal laboratory to address this problem. One important success is the understanding of the nature of the quenched approximation [6]. Below, we will discuss the phase structure of chRMT by means of the distribution of Yang-Lee zeros [20].

## 2. The Chiral order parameter

The order parameter of the chiral phase transition,  $\langle \bar{\psi}\psi \rangle$ , is nonzero only below the critical temperature. As was shown in [7]  $\langle \bar{\psi}\psi \rangle$  is directly related to the eigenvalue density of the QCD Dirac operator per unit four-volume

$$\Sigma \equiv |\langle \bar{\psi}\psi \rangle| = \frac{\pi \langle \rho(0) \rangle}{V}. \quad (1)$$

It is elementary to derive this relation. The Euclidean Dirac operator for gauge field configuration  $A_\mu$  is given by  $D = \gamma_\mu(\partial_\mu + iA_\mu)$ . For Hermitean gamma matrices  $D$  is anti-hermitean with purely imaginary eigenvalues,  $D\phi_k = i\lambda_k\phi_k$ , and spectral density given by  $\rho(\lambda) = \sum_k \delta(\lambda - \lambda_k)$ . Because  $\{\gamma_5, D\} = 0$ , nonzero eigenvalues occur in pairs  $\pm\lambda_k$ . In terms of the eigenvalues of  $D$  the QCD partition function for  $N_f$  flavors of mass  $m$  can then be written as

$$Z(m) = \langle \prod_k (\lambda_k^2 + m^2)^{N_f} \rangle, \quad (2)$$

where the average  $\langle \cdot \rangle$  is over all gauge field configurations weighted according to the Euclidean action.

The chiral condensate follows immediately from the partition function (2),

$$\langle \bar{\psi}\psi \rangle = \frac{1}{VN_f} \partial_m \log Z(m) = \frac{1}{V} \langle \sum_k \frac{2m}{\lambda_k^2 + m^2} \rangle. \quad (3)$$

If we express the sum as an integral over the spectral density, and take the thermodynamic limit before the chiral limit so that we have many eigenvalues less than  $m$  we recover (1) (Notice the order of the limits.).

Another way to characterize the chiral condensate is via the zeros of the partition function [21,22]. For a finite number of degrees of freedom  $Z(m)$  can be factorized as  $Z(m) \sim \prod_k (m - m_k)$ . The chiral condensate is then given by

$$\langle \bar{\psi} \psi \rangle = \frac{1}{VN_f} \partial_m \log Z(m) = \frac{1}{V} \sum_k \frac{1}{m - m_k}. \quad (4)$$

In the chirally broken phase zeros are located on a segment of the imaginary axis that includes  $m = 0$ . In the thermodynamic limit they coalesce into a cut and the chiral condensate shows a discontinuity each time  $m$  crosses this cut. In the chirally symmetric phase, we expect to find a cut *away* from the imaginary axis.

The eigenvalues of the Dirac operator  $D = \gamma_\mu (\partial_\mu + iA_\mu) + \gamma_0 \mu$  at nonzero chemical potential are scattered in the complex plane (see for example [5]). For a finite number of degrees of freedom the partition function,  $Z(m, \mu)$ , is a polynomial in  $m$  and  $\mu$ . The condensate can be related to either to the spectral density or to the zeros of  $Z(m, \mu)$ . An alternative order parameter is the baryon density  $n_B = \partial_\mu \log Z(m, \mu) / N_f V$ . We can differentiate with respect to  $\mu$  before or after averaging over the gauge fields. In the first case the baryon number density follows from the spectral density of  $\gamma_0(D + m)$  with eigenvalues scattered in the complex plane. In the second case the baryon number density follows from the zeros of  $Z(m, \mu)$  in the complex  $\mu$  plane.

### 3. The Dirac Spectrum

An important consequence of the Banks-Casher formula (1) is that the eigenvalues near zero virtuality are spaced as  $\Delta\lambda = 1/\rho(0) = \pi/\Sigma V$ . This should be contrasted with the eigenvalue spectrum of the non-interacting Dirac operator. Then  $\rho^{\text{free}}(\lambda) \sim V\lambda^3$  which leads to an eigenvalue spacing of  $\Delta\lambda \sim 1/V^{1/4}$ . Clearly, the presence of gauge fields lead to a strong modification of the spectrum near zero virtuality. Strong interactions result in the coupling of many degrees of freedom leading to extended states and correlated eigenvalues. On the other hand, for uncorrelated eigenvalues, the eigenvalue distribution factorizes and we have  $\rho(\lambda) \sim \lambda^{2N_f+1}$ , i.e. no breaking of chiral symmetry.

Numerous studies have shown that spectral correlations of complex systems on a scale set by the level spacing are universal, i.e. they do not depend on the dynamics of the system and are completely determined by symmetries. Because the QCD Dirac spectrum is symmetric about zero, we have two different

types of eigenvalue correlations: correlations in the bulk of the spectrum and spectral correlations near zero virtuality. In the context of chiral symmetry we wish to study the spectral density near zero virtuality. Because the eigenvalues are spaced as  $1/\Sigma V$  it is natural to introduce the microscopic spectral density

$$\rho_S(u) = \lim_{V \rightarrow \infty} \frac{1}{V\Sigma} \rho\left(\frac{u}{V\Sigma}\right). \quad (5)$$

The dependence on the macroscopic variable  $\Sigma$  has been eliminated and therefore  $\rho_S(u)$  is a perfect candidate for a universal function.

#### 4. Spectral universality

Spectra for a wide range of complex quantum systems have been studied both experimentally [23–25] and numerically [8,26,27]. One basic observation has been that the scale of variations of the average spectral density and the scale of the spectral fluctuations separate. This allows us to unfold the spectrum, i.e. we rescale the spectrum in units of the local average level spacing. The fluctuations of the unfolded spectrum can be measured by suitable statistics. We will consider the nearest neighbor spacing distribution,  $P(S)$ , the number variance,  $\Sigma_2(n)$ , and the  $\Delta_3(n)$  statistic. The number variance is defined as the variance of the number of levels in a stretch of the spectrum that contains  $n$  levels on average, and  $\Delta_3(n)$  is obtained from  $\Sigma_2(n)$  by averaging over a smoothening kernel.

These statistics can be obtained analytically for the invariant random matrix ensembles (see [8,28]) defined as ensembles of Hermitean matrices with independently distributed Gaussian matrix elements. Depending on the anti-unitary symmetry, the matrix elements are real, complex or quaternion real. The corresponding Dyson index is given by  $\beta = 1, 2$ , and  $4$ , respectively. The nearest neighbor spacing distribution is given by  $P(S) \sim S^\beta \exp(-a_\beta S^2)$ . The asymptotic behavior of  $\Sigma_2(n)$  and  $\Delta_3(n)$  is given by  $\Sigma_2(n) \sim (2/\pi^2\beta) \log(n)$  and  $\Delta_3(n) \sim \beta \Sigma_2(n)/2$ . For uncorrelated eigenvalues one finds that  $P(S) = \exp(-S)$ ,  $\Sigma_2(n) = n$  and  $\Delta_3(n) = n/15$ . Characteristic features of random matrix correlations are level repulsion at short distances and a strong suppression of fluctuations at large distances.

Numerous studies have shown that the spectral correlations of a classically chaotic systems are given by RMT. This conjecture has been strengthened by recent analytical arguments [29–31] and universality arguments [32].

#### 5. Chiral random matrix theory

In this section we will introduce an instanton liquid inspired [33] RMT for the QCD partition function. In the spirit of the invariant random matrix ensembles

we construct a model for the Dirac operator with the global symmetries of the QCD partition function as input, but otherwise Gaussian random matrix elements. The chRMT that obeys these conditions is defined by [34–36]

$$Z_\nu^\beta = \int DW \prod_{f=1}^{N_f} \det(\mathcal{D} + m_f) e^{-\frac{N\Sigma^2\beta}{4}\text{Tr}W^\dagger W}, \quad \text{with} \quad \mathcal{D} = \begin{pmatrix} 0 & iW \\ iW^\dagger & 0 \end{pmatrix}, \quad (6)$$

and  $W$  is a  $n \times m$  matrix with  $\nu = |n - m|$  and  $N = n + m$ . The matrix elements of  $W$  are either real ( $\beta = 1$ , chiral Gaussian Orthogonal Ensemble (chGOE)), complex ( $\beta = 2$ , chiral Gaussian Unitary Ensemble (chGUE)), or quaternion real ( $\beta = 4$ , chiral Gaussian Symplectic Ensemble (chGSE)).

This model reproduces the following symmetries of the QCD partition function: *i*) The  $U_A(1)$  symmetry. All nonzero eigenvalues of the random matrix Dirac operator occur in pairs  $\pm\lambda$ . *ii*) The topological structure of the QCD partition function. The Dirac matrix has exactly  $|\nu| \equiv |n - m|$  zero eigenvalues. This identifies  $\nu$  as the topological sector of the model. *iii*) The flavor symmetry is the same as in QCD [37]. *iv*) The chiral symmetry is broken spontaneously with chiral condensate given by  $\Sigma = \lim_{N \rightarrow \infty} \pi\rho(0)/N$ . ( $N$  is interpreted as the (dimensionless) volume of space time.) *v*) The anti-unitary symmetries. For fundamental fermions the matrix elements of the Dirac operator are complex for  $N_c \geq 3$  ( $\beta = 2$ ) but can be chosen real for  $N_c = 2$  ( $\beta = 1$ ). For adjoint fermions they can be arranged into real quaternions ( $\beta = 4$ ).

The ensemble of matrices in (6) is also known as the Laguerre ensemble. Note that its spectral correlations in the bulk of the spectrum are given by the invariant random matrix ensemble with the same value of  $\beta$  [38]. Both types of microscopic correlations are stable against deformations of the ensemble. This has been shown by a variety of different arguments [39–42].

Below we will discuss the microscopic spectral density. For  $N_c = 3$ ,  $N_f$  flavors and topological charge  $\nu$  it is given by [35]

$$\rho_S(u) = \frac{u}{2} \left( J_a^2(u) - J_{a+1}(u)J_{a-1}(u) \right), \quad (7)$$

where  $a = N_f + \nu$ . The result for  $N_c = 2$ , which is more complicated, is given in [43], and the result for the symplectic ensemble is derived in [44].

Together with the invariant random matrix ensembles, the chiral ensembles are part of a larger classification scheme. As pointed out in [45], there is a one to one correspondence between random matrix theories and symmetric spaces.

## 6. Lattice QCD results

Recently, Kalkreuter [46] calculated *all* eigenvalues of the lattice Dirac operator both for Kogut-Susskind (KS) fermions and Wilson fermions for lattices

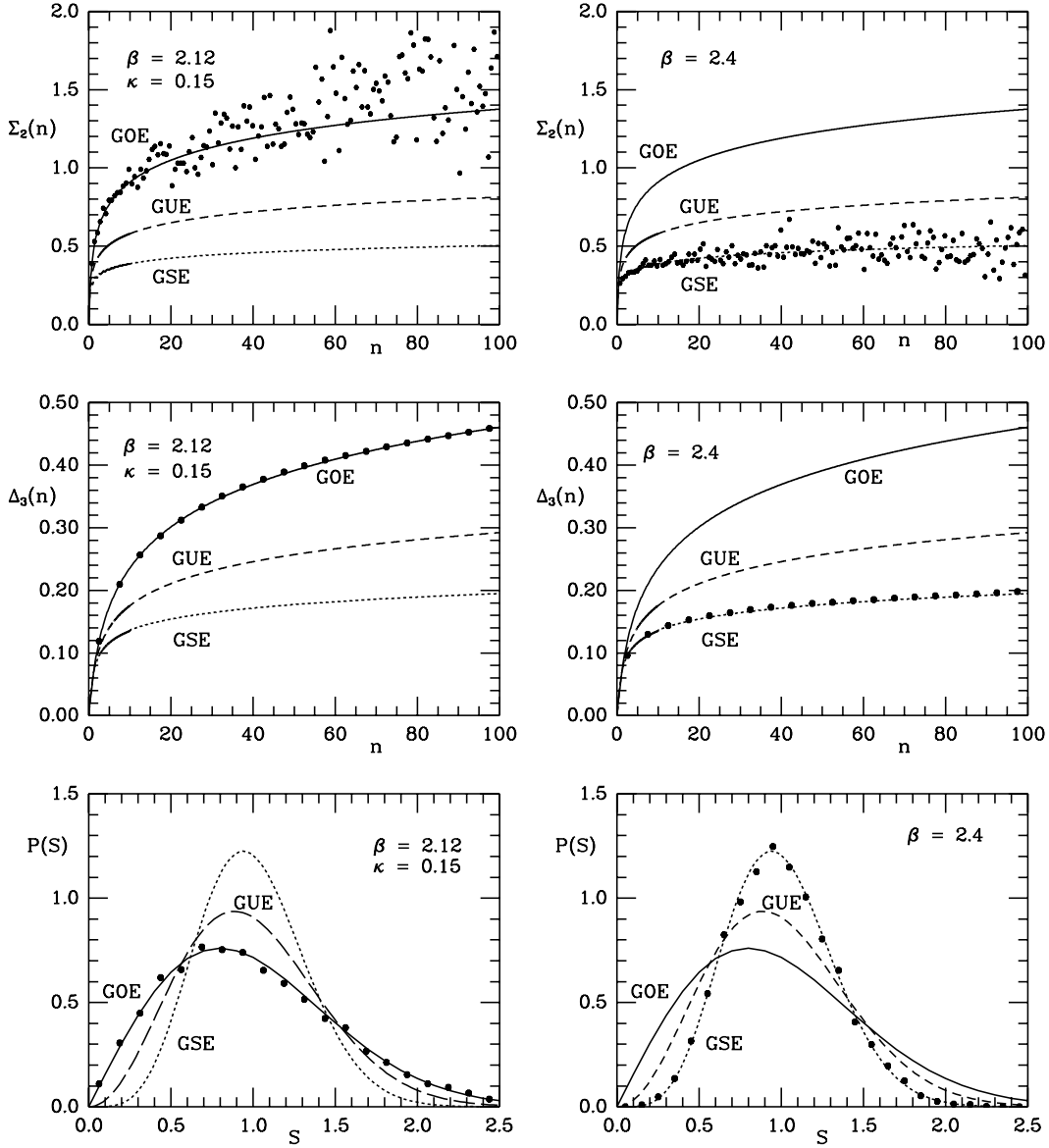


Fig. 1. Spectral correlations of Dirac eigenvalues for Wilson fermions (upper) and KS-fermions (lower).

as large as  $12^4$ . In the the case of  $SU(2)$  the anti-unitary symmetry of the KS and the Wilson Dirac operator is different [47,48]. For KS fermions the Dirac matrix can be arranged into real quaternions, whereas the *Hermitean* Wilson Dirac matrix  $\gamma_5 D^{\text{Wilson}}$  can be chosen real. Therefore, we expect that the

eigenvalue correlations are described by the GSE and the GOE, respectively [48]. In Fig. 1 we show results for  $\Sigma_2(n)$ ,  $\Delta_3(n)$  and  $P(S)$ . The results for KS fermions are for 4 dynamical flavors with  $ma = 0.05$  on a  $12^4$  lattice. The results for Wilson fermion were obtained for two dynamical flavors on a  $8^3 \times 12$  lattice. Other statistics are discussed in [49].

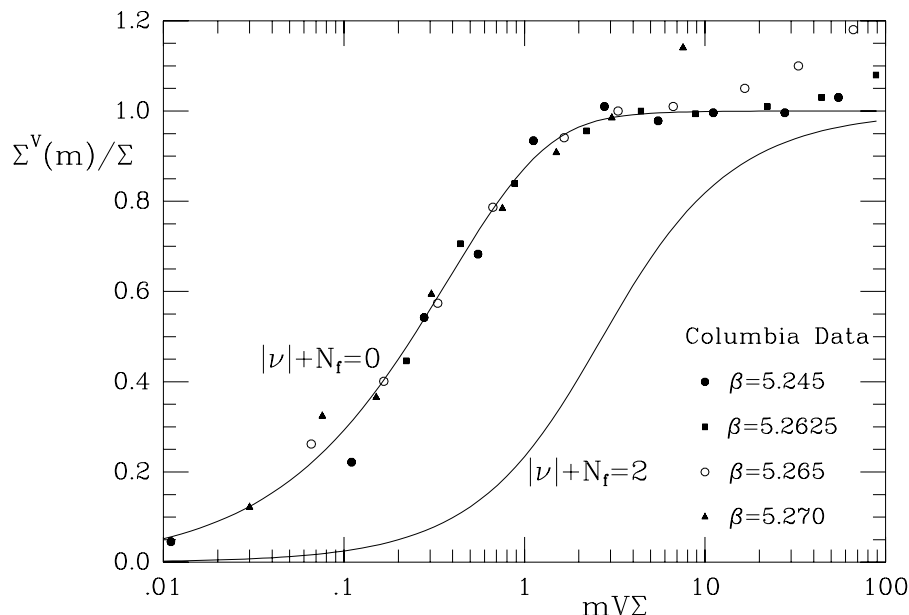


Fig. 2. The valence quark mass dependence of the chiral condensate.

Lattice studies of the microscopic spectral density are in progress and preliminary results are promising [50]. However, an alternative way to probe the Dirac spectrum was introduced by the Columbia group [51]. They studied the valence quark mass dependence of the Dirac operator, i.e.  $\Sigma(m) = \frac{1}{N} \int d\lambda \rho(\lambda) 2m / (\lambda^2 + m^2)$ , for a fixed sea quark mass. In the mesoscopic range, the valence quark mass dependence can be obtained analytically from the microscopic spectral density (7) [52],

$$\frac{\Sigma(x)}{\Sigma} = x(I_a(x)K_a(x) + I_{a+1}(x)K_{a-1}(x)), \quad (8)$$

where  $x = mV\Sigma$  is the rescaled mass and  $a = N_f + \nu$ . In Fig. 2 we plot this ratio as a function of  $x$  for lattice data of two dynamical flavors with mass

$ma = 0.01$  and  $N_c = 3$  on a  $16^3 \times 4$  lattice. We observe that the lattice data for different values of  $\beta$  fall on a single curve. Moreover, in the mesoscopic range this curve coincides with the random matrix prediction for  $N_f = \nu = 0$ . Apparently, the zero modes are completely mixed with the much larger number of nonzero modes. For eigenvalues much smaller than the sea quark mass, we expect to see the  $N_f = 0$  eigenvalue correlations.

## 7. Chiral random matrix model at nonzero chemical potential

At nonzero temperature and chemical potential the random matrix Dirac operator in 6 is given by [53–55]

$$\mathcal{D} = \begin{pmatrix} 0 & iW + i\Omega_T + \mu \\ iW^\dagger + i\Omega_T + \mu & 0 \end{pmatrix}, \quad (9)$$

where  $\Omega_T = T \otimes_n (2n + 1)\pi \mathbf{1}$ .

Inspired by [56], the simplest model is obtained by keeping only the lowest Matsubara frequency [53,54]. We wish to stress that this model is a *schematic* model of the QCD partition function. Below, we will discuss a model with  $\Omega_T$  absorbed by the random matrix and  $\mu \neq 0$ . Then the eigenvalues of  $\mathcal{D}$  are scattered in the complex plane. In the quenched approximation its distribution was obtained analytically [6] from the  $N_f \rightarrow 0$  limit of a partition function with the determinant replaced by its absolute value. To this end the RMT partition function was rewritten in terms a  $\sigma$ -model amenable to a saddle point approximation. The  $\sigma$ -model shows a second order phase transition at the boundary of the spectrum leading to a vanishing curvature and a diverging two point function. This was confirmed by an explicit calculation of this two-point function in [57].

In the remainder of this section we consider the *unquenched* partition function for one flavor. Using a multi-precision package [58], we have calculated the (Yang-Lee) zeros of the partition function in the complex  $\mu$  and  $m$  plane for values of  $n$  as large as 192. Results for  $n = 192$  are shown in Fig. 3. Notice that the zeros fall on a curve [59].

From a saddle-point analysis it can be shown that for zero mass the model shows a first order phase transition along the curve  $\text{Re}[\mu^2 + \log(\mu^2)] = -1$  [6,60]. The discontinuity of  $n_B$  requires that the zeros of the partition function fall along this curve (see left upper figure). At the endpoints (stars) two different solutions of the saddle point equation (a cubic equation [53]) coalesce. All other curves can be obtained from a saddle-point analysis as well. A schematic picture of the phase structure in the complex  $m$  plane is shown in [61].

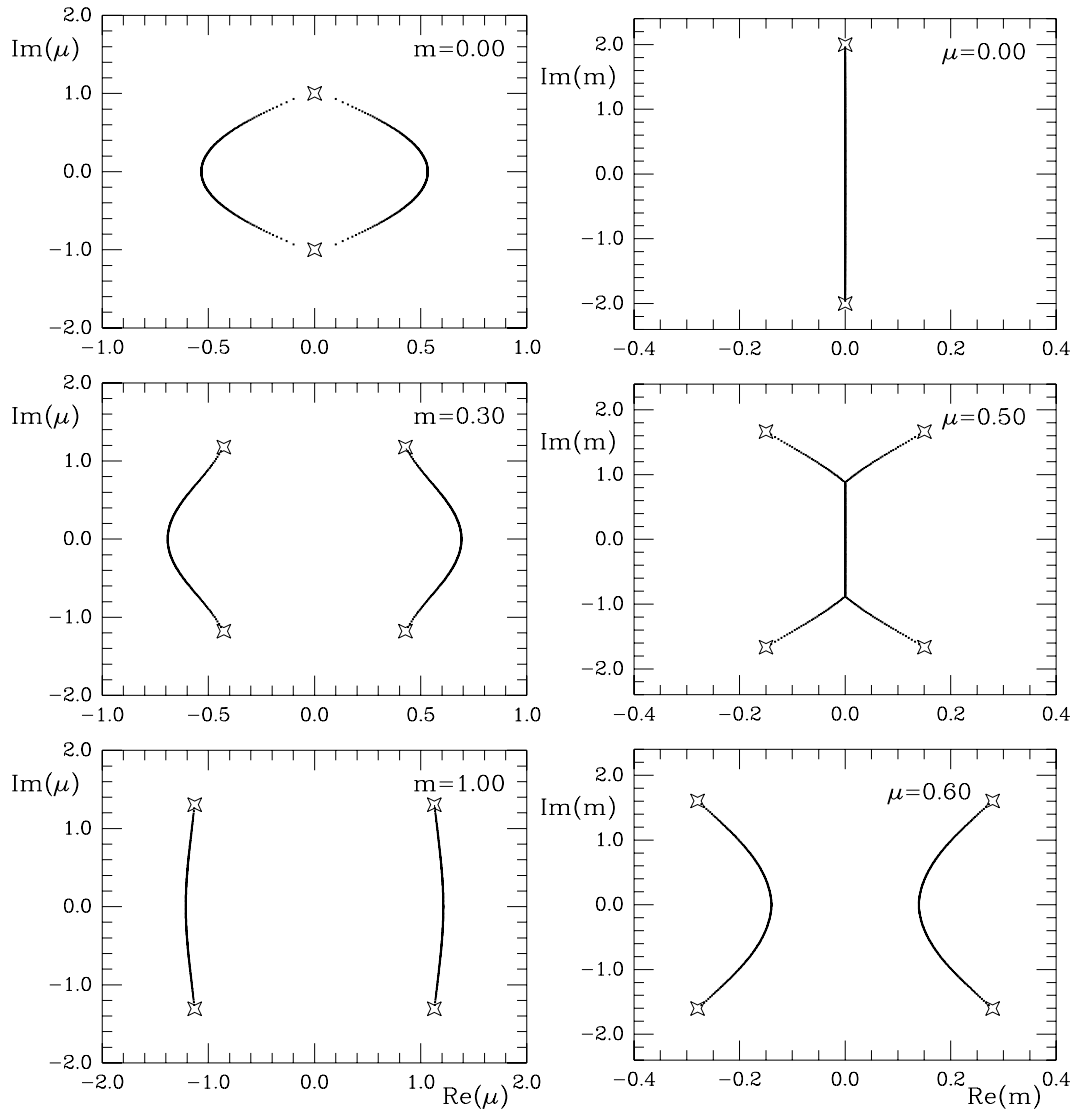


Fig. 3. Zeros of the partition function in the complex  $m$  and  $\mu$  plane.

## 8. Conclusions

We have shown that the microscopic correlations of the QCD Dirac spectrum can be explained by RMT and have obtained an analytical understanding of the distribution of the eigenvalues closest to zero. We have given an extension of this model to nonzero temperature and chemical potential. Its phase structure has been mapped out unambiguously by means of Yang-Lee zeros.

This work was partially supported by the US DOE grant DE-FG-88ER40388. M.A. Halasz is thanked for a critical reading of the manuscript.

## REFERENCES

1. C. DeTar, *Quark-gluon plasma in numerical simulations of QCD*, in *Quark gluon plasma 2*, R. Hwa ed., World Scientific 1995.
2. A. Ukawa, Lattice 1996, hep-lat/9612011.
3. C. Bernard, T. Blum, C. DeTar, S. Gottlieb, U. Heller, J. Hetrick, K. Rummukainen, R. Sugar, D. Toussaint and M. Wingate, Phys. Rev. Lett. **78** (1997) 598.
4. I. Barbour, S. Morrison and J. Kogut, hep-lat/9612012.
5. I. Barbour, N. Behihil, E. Dagotto, F. Karsch, A. Moreo, M. Stone and H. Wyld, Nucl. Phys. **B275** (1986) 296; M. Lombardo, J. Kogut and D. Sinclair, hep-lat/9511026.
6. M. Stephanov, Phys. Rev. Lett. **76** (1996) 4472.
7. T. Banks and A. Casher, Nucl. Phys. **B169** (1980) 103.
8. O. Bohigas, M. Giannoni, Lecture notes in Physics **209** (1984) 1.
9. W. Hauser and H. Feshbach, Phys. Rev. **87** (1952) 366; J. Verbaarschot, H. Weidenmüller and M. Zirnbauer, Phys. Rep. **129** (1985) 367.
10. R. Denton, B. Mühlischlegel and D. Scalapino, Phys. Rev. Lett. **26** 1971.
11. C. Beenakker, Rev. Mod. Phys. (1997), cond-mat/9612179.
12. Y. Imry, Europhysics Lett. **1** (1986) 249; S. Iida, H. Weidenmüller and J. Zuk, Phys. Rev. Lett. **64** (1990) 583; Ann. Phys. (N.Y.) **200** (1990), 219.
13. H. Leutwyler and A. Smilga, Phys. Rev. **D46** (1992) 5607.
14. D. Voiculescu, K. Dykema and A. Nica, *Free Random Variables*, Am. Math. Soc., Providence RI, 1992.
15. A. Zee, Nucl. Phys. **B474** (1996) 726.
16. M. Engelhardt and S. Levit, hep-th/9609216.
17. R. Janik, M. Nowak, G. Papp, J. Wambach, and I. Zahed, hep-ph/9609491.
18. P. Anderson, Phys. Rev. **109** (1958) 1492.
19. D. Gross and E. Witten, Phys. Rev. **D21** (1980) 446; S. Chandrasekharan, hep-th/9610225. H. Sommers, A. Crisanti, H. Sompolinsky and Y. Stein, Phys. Rev. Lett. **60** (1988) 1895.
20. C.N. Yang and T.D. Lee, Phys. Rev. **87** (1952) 104, 410.
21. J. Vink, Nucl. Phys. **B323** (1989) 399.
22. I. Barbour, A. Bell, M. Bernaschi, G. Salina and A. Vladikas, Nucl. Phys. B386 (1992) 683.
23. R. Haq, A. Pandey and O. Bohigas, Phys. Rev. Lett. **48** (1982) 1086.
24. C. Ellegaard, T. Guhr, K. Lindemann, H.Q. Lorensen, J. Nygård and M.

Oxborrow, Phys. Rev. Lett. **75** (1995) 1546.

25. S. Deus, P. Koch and L. Sirko, Phys. Rev. **E 52** (1995) 1146; H. Gräf, H. Harney, H. Lengeler, C. Lewenkopf, C. Rangacharyulu, A. Richter, P. Schardt and H. Weidenmüller, Phys. Rev. Lett. **69** (1992) 1296.

26. T. Seligman, J. Verbaarschot, and M. Zirnbauer, Phys. Rev. Lett. **53**, 215 (1984); T. Seligman and J. Verbaarschot, Phys. Lett. **108A** (1985) 183.

27. S. Drozdz, A. Trellakis and J. Wambach, Phys. Rev. Lett. **76** (1996) 4891.

28. F. Dyson and M. Mehta, J. Math. Phys. **4** (1963) 701.

29. M. Berry, Proc. Roy. Soc. London **A 400** (1985) 229.

30. A. Andreev, O. Agam, B.D. Simons and B.L. Altshuler, cond-mat/9605204.

31. A. Altland and M. Zirnbauer, Phys. Rev. Lett. **77** (1996) 4536.

32. A. Pandey, Ann. Phys. **134** (1981) 119; J. Ambjorn, J. Jurkiewicz and Y. Makeenko, Phys. Lett. B251 (1990) 517; E. Brézin and A. Zee, Nucl. Phys. **B402** (1993) 613; C. Beenakker, Nucl.Phys. **B422** (1994) 515; G. Hackenbroich and H. Weidenmüller, Phys. Rev. Lett. **74** (1995) 4118; S. Higuchi, C.Itoi, S.M. Nishigaki and N. Sakai, hep-th/9612237.

33. T. Schäfer and E. Shuryak, Rev. Mod. Phys. (1997), hep-ph/9610451.

34. E. Shuryak and J. Verbaarschot, Nucl. Phys. **A560** (1993) 306.

35. J. Verbaarschot, Phys. Rev. Lett. **72** (1994) 2531; Phys. Lett. **B329** (1994) 351; Nucl. Phys. **B427** (1994) 434.

36. J. Verbaarschot and I. Zahed, Phys. Rev. Lett. **70** (1993) 3852.

37. A. Smilga and J. Verbaarschot, Phys. Rev. **D51** (1995) 829; M. Halasz and J. Verbaarschot, Phys. Rev. **D52** (1995) 2563.

38. D. Fox and P.Kahn, Phys. Rev. **134** (1964) B1152; (1965) 228; T. Nagao and M. Wadati, J. Phys. Soc. Jap. **60** (1991) 3298, **61** (1992) 78, 1910.

39. E. Brézin, S. Hikami and A. Zee, Nucl. Phys. **B464** (1996) 411.

40. A. Jackson, M. Sener and J. Verbaarschot, Nucl. Phys. **B479** [FS] (1996) 707.

41. S. Nishigaki, Phys. Lett. B (1996); G. Akemann, P. Damgaard, U. Magnea and S. Nishigaki, hep-th/9609174.

42. J. Ambjorn and G. Akeman, J. Phys. A29 (1996) L555; Nucl. Phys. **B482** (1996) 403.

43. J. Verbaarschot, Nucl. Phys. B426 (1994) 559.

44. T. Nagao and P.J. Forrester, Nucl. Phys. **B435** (1995) 401.

45. F. Dyson, Comm. Math. Phys. **19** (1970) 235; A. Altland, M. Zirnbauer, Phys. Rev. Lett. **76** (1996) 3420; M. Zirnbauer, J. Math. Phys. **37** (1996) 4986; M.Caselle, cond-mat/9610017.

46. T. Kalkreuter, Comp. Phys. Comm. **95** (1996) 1; Phys. Lett. **B276** (1992)

485; Phys. Rev. **D48** (1993) 1926.

- 47. S. Hands and M. Teper, Nucl. Phys. **B347** (1990) 819.
- 48. M. Halasz and J. Verbaarschot, Phys. Rev. Lett. **74** (1995) 3920.
- 49. M. Halasz, T. Kalkreuter and J. Verbaarschot, hep-lat/9607042, Lattice 1996.
- 50. S. Meyer, private communication; T. Wettig, T. Guhr, A. Schäfer and H. Weidenmüller, hep-ph/9701387 (this proceedings).
- 51. S. Chandrasekharan, Lattice 1994, 475; S. Chandrasekharan and N. Christ, Lattice 1995, 527; N. Christ, Lattice 1996.
- 52. J. Verbaarschot, Phys. Lett. **B368** (1996) 137.
- 53. A. Jackson and J. Verbaarschot, Phys. Rev. **D53** (1996) 7223.
- 54. T. Wettig, A. Schäfer and H. Weidenmüller, Phys. Lett. **B367** (1996) 28.
- 55. M. Stephanov, Phys. Lett. **B275** (1996) 249.
- 56. A. Kocic and J. Kogut, Nucl. Phys. **B455** (1995) 229.
- 57. R. Janik, M. Nowak, G. Papp and I. Zahed, Phys. Rev. Lett. **77** (1996) 4876.
- 58. D. Bailey, NASA Ames RNR Technical Report RNR-94-013.
- 59. V. Mattheev and R. Shrock, J. Phys. A: Math. Gen. **28** (1995) 5235.
- 60. M. Halasz, A. Jackson and J. Verbaarschot, Phys. Lett. **B** (1997); in preparation.
- 61. M. Stephanov, hep-lat/9607060, Lattice 1996.